Experimental observations of nonlinear effects in waves in a nonneutral plasma

Grant W. Hart, Ross L. Spencer, and Bryan G. Peterson

Citation: AIP Conference Proceedings **498**, 182 (1999); doi: 10.1063/1.1302118
View online: http://dx.doi.org/10.1063/1.1302118
View Table of Contents:
http://scitation.aip.org/content/aip/proceeding/aipcp/498?ver=pdfcov
Published by the AIP Publishing

Experimental Observations of Nonlinear Effects in Waves in a Nonneutral Plasma

Grant W. Hart, Ross L. Spencer and Bryan G. Peterson

Department of Physics and Astronomy
Brigham Young University

Abstract. We have been making measurements of nonlinear effects that occur in the normal modes of electrostatic waves in a pure electron plasma. The two effects described here are (1) mode coupling between normal modes and (2) formation of solitons from the normal modes. The coupling between the modes in the plasma occurs because of the nonlinear terms in the continuity and momentum equations. We see the coupling between the $n_z = 1$ and $n_z = 2$ modes in our plasma, where n_z is the number of half-wavelengths that fit into the plasma. These are the only two modes that have close enough frequency matching to couple significantly. The predicted amplitude and phase dependence of this coupling theory are verified in our data.

When normal modes are grown to large amplitudes, they can become solitons bouncing between the ends of the system. We have measured these solitons and have shown that they have the expected properties of solitons: when not interacting, they travel faster than the linear wave speed in the plasma and they also show the phase delay expected when they interact with each other. Because of the interaction between the height of the soliton and its speed, solitons can only be grown from normal modes in a limited amplitude range. Mode coupling can come into play with these solitons and even cause one to disappear.

INTRODUCTION

We have been studying electrostatic Trivelpiece-Gould modes in a nonneutral plasma confined in a Malmberg-Penning trap [1]. Our plasma is 60 cm long and about 2 cm in radius. The plasma temperature is about 1 eV [2]. The waves that we have been studying have had large enough amplitudes that nonlinear effects become important. There are two main nonlinear effects that we have observed: (1) Coupling between different modes and (2) Solitons.

MODE COUPLING

The mode coupling we observe occurs between the lowest frequency standing waves. Because of our long, thin geometry these are basically Trivelpiece-Gould

CP498, *Non-Neutral Plasma Physics III,* edited by John J. Bollinger, et al.

modes with close to an integral number of half-wavelengths in the plasma [3,4]. We identify these modes by their n_z value, which can be defined as the number of half-wavelength in the plasma. The lowest frequency mode has $^1/_2$ wavelength in the plasma, so it has an n_z of 1. It has odd symmetry relative to the center of the plasma. The next higher mode has one full wavelength in the plasma, so it has an n_z of 2. It has even symmetry relative to the center of the plasma.

Physical Mechanism of mode coupling

Product terms, such as $\nabla \cdot (n\mathbf{v})$ in the continuity equation and $\mathbf{v} \cdot \nabla \mathbf{v}$ in the momentum equation can create a drive for other modes, because they involve the sum and difference frequencies. If the drive from these terms matches a mode's structure both spatially and temporally, then the driven mode can either grow or shrink, depending on the phase relationship between the mode and the drive.

For example, if we have mostly the $n_z = 2$ mode with just a little bit of the $n_z = 1$ mode present, this can cause the $n_z = 1$ mode to grow to large amplitude.

Simple theory

Assume modes of the form

$$n_1 = n_{10} \sin(\omega_1 t) \sin(k_1 z) \tag{1}$$

$$n_2 = n_{20} \sin(\omega_2 t + \phi) \cos(k_2 z) \tag{2}$$

the corresponding velocities are

$$v_1 = \frac{n_{10}}{n_0} \frac{\omega_1}{k_1} \cos(\omega_1 t) \cos(k_1 z) \tag{3}$$

$$v_2 = -\frac{n_{20}}{n_0} \frac{\omega_2}{k_2} \cos(\omega_2 t + \phi) \sin(k_2 z) \tag{4}$$

We put these into the continuity equation and find the terms that have the same spatial and temporal dependence as the n_1 and n_2 modes. The result is that

$$\frac{\partial n_{10}}{\partial t} = \frac{n_{10} n_{20}}{2 n_0} \omega_1 \cos\phi \tag{5}$$

$$\frac{\partial n_{20}}{\partial t} = -\frac{n_{10}^2}{2 n_0} \omega_1 \cos\phi. \tag{6}$$

Note that if the phase is in the right range the first equation leads to initial exponential growth for the $n_z = 1$ mode. If there is a small frequency mismatch between the two modes, we define $\delta\omega = \omega_2 - 2\omega_1$. We can model this by having a time dependent phase, $\phi = \phi_0 + \delta\omega t$ in the above equations and it leads to alternate periods of growth and decay.

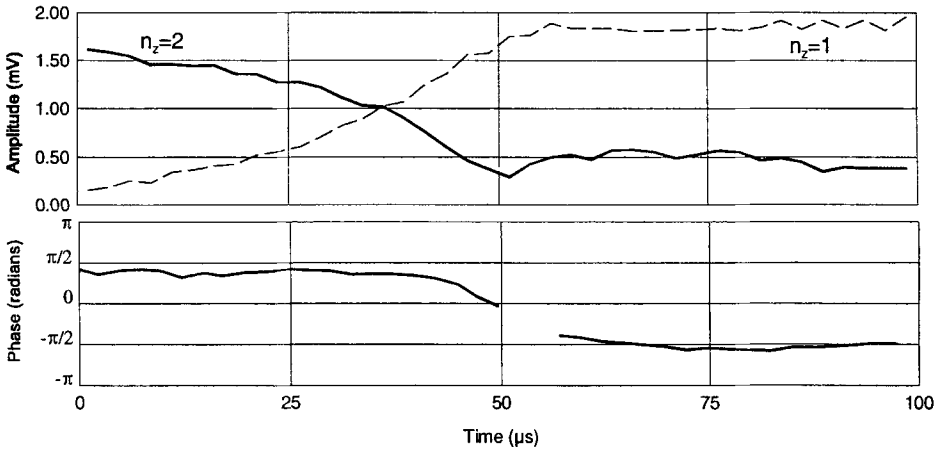

FIGURE 1. Mode conversion for 1 Volt drive. The upper plot shows the amplitude of the two modes as a function of time. The lower plot shows the relative phase between the two modes.

Experimental Measurements

We launch these modes by oscillating the confining potentials at the end of the plasma at the $n_z = 2$ mode frequency. For these experiments we applied the same oscillating potential to both ends, matching the even symmetry of the mode.

We observe the modes by measuring the image charge induced on the wall rings. The amount of charge induced on an azimuthally symmetric ring is close to the total charge under the ring, so what we measure is approximately

$$\int_{z_{beg}}^{z_{end}} n \, dz. \tag{7}$$

Note that if a mode has a node centered under a ring, then we are insensitive to that mode on that ring.

We recorded our data on two rings centered at ± 20 cm away from the center of the plasma, approximately $^2/_3$ of the way from the center of the plasma to its end. The rings were 10 cm long. It should be noted that this configuration is insensitive to the $n_z = 3$ mode because of the ring placement relative to the nodes of that mode. The signals for the n_z=1 and n_z=2 modes can be separated by adding and subtracting these two signals because of the symmetry of the modes. We observe the image charge on these rings after the drive has stopped.

Figure 1 shows the amplitude of the two modes as a function of time when the driving voltage is one volt. Note that the amplitude of the n_z=1 mode grows and the n_z=2 mode goes to a smaller (but nonzero) value. The phase approaches $-\frac{\pi}{2}$. When the phase is $\pm\frac{\pi}{2}$, the mode conversion will stop because of the $\cos\phi$ dependence in

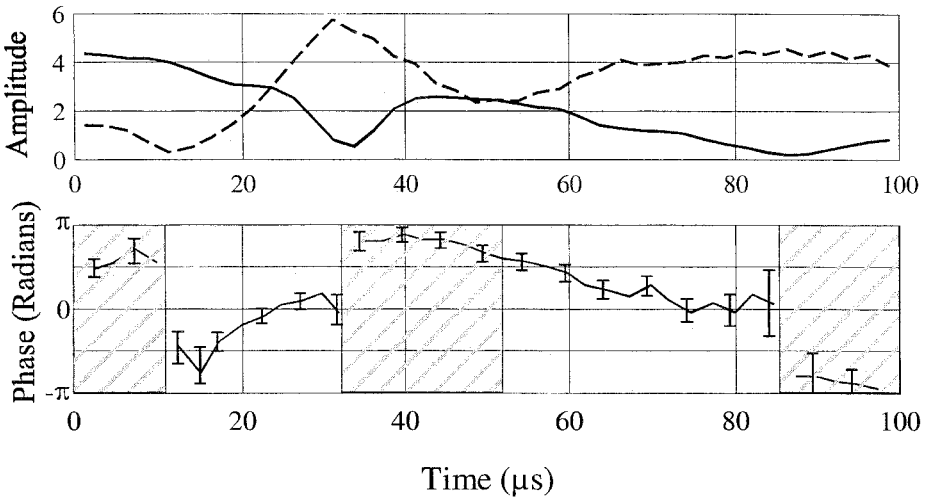

FIGURE 2. Mode conversion for 2 Volt drive. The upper plot shows the amplitude of the two modes as a function of time. The lower plot shows the relative phase between the two modes. The shaded regions show the times when the $n_z = 1$ mode is shrinking and the $n_z = 2$ mode is growing.

equations 5 and 6. All of our one-volt data shows the phase eventually going to one of these values.

Figure 2 shows the amplitude of the two modes when the driving voltage is two volts. In this case we get conversion back and forth between the two modes as the relative phase varies due to the frequency mismatch. Equations 5 and 6 predict growth for the $n_z = 1$ mode when $\cos\phi$ is in the range from $-\frac{\pi}{2}$ to $\frac{\pi}{2}$ and damping when outside that range. The shaded areas on the lower curve in Figure 2 are the times when the phase should be outside of that range, based on the growth or damping of the modes. We can see that within the error bars this prediction is correct.

In order go beyond the qualitative result shown above, we need to verify that the growth of the $n_z = 1$ mode has the proper $\cos\phi$ dependence. The left hand plot of Figure 3 shows the growth rate of the $n_z = 1$ mode with the n_{20} dependence divided out plotted versus $\cos\phi$. This fits a linear curve very nicely, showing the predicted $\cos\phi$ dependence. We can also take the same data and plot it versus the amplitude of the $n_z = 2$ mode, since this should also be linear when the ϕ dependence is removed. The right hand plot of Figure 3 shows this plot, which is also linear. The slopes of these lines should depend only on n_0 and ω_1, but there appears to be some variation between shots of different drive amplitude that is not yet understood.

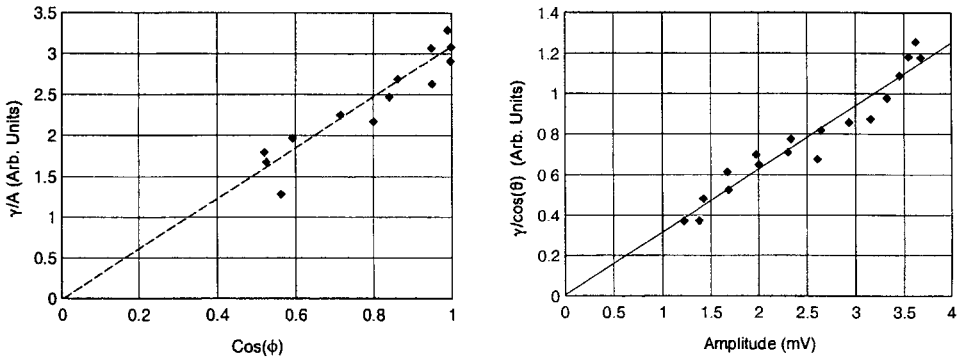

FIGURE 3. Phase and Amplitude dependence of mode growth. The figure on the left shows that γ/A is proportional to $\cos\theta$. The figure on the right shows that $\gamma/\cos\theta$ is proportional to A.

Energy transfer

The small signal energy density of these modes can be shown to be

$$u = \epsilon_0 E_z^2 \left(1 + \frac{\omega_p^2}{\omega^2}\right)$$

The connection between E_z and the voltage that we measure on the rings can be obtained by recognizing that the voltage is proportional to the charge under the rings, as in Equation 7. n can be obtained by recognizing that in this geometry the radial part of ∇^2 dominates in Poisson's equation. This makes the electric potential proportional to n, *independent of the frequency* for low frequency modes. Therefore, E_z is proportional to $\frac{n}{\lambda}$ or $n\omega$. Since both modes are integrated over an integer number of half-wavelengths, the total mode energy can be written as

$$\text{Energy} \propto n^2\omega^2 \left(1 + \frac{\omega_p^2}{\omega^2}\right)$$

Using this result to plot the energy transfered between the two modes in the two volt case shown above, we get Figure 4. We can see that the energy initially drops due to the damping of the $n_z = 2$ mode. This levels out as energy gets stored in the $n_z = 1$ mode, which has much less damping. When the system converts back to the $n_z = 2$ mode, the energy again decays until the system ends up back in the $n_z = 1$ state. The wiggles in the energy curve at about 25 and 40 μsec might correspond to energy being coupled into and out of the $n_z = 3$ mode. The frequency of the wiggles roughly corresponds to the frequency mismatch between these modes, but we are unable to measure the $n_z = 3$ mode directly because of the placement of the measuring rings.

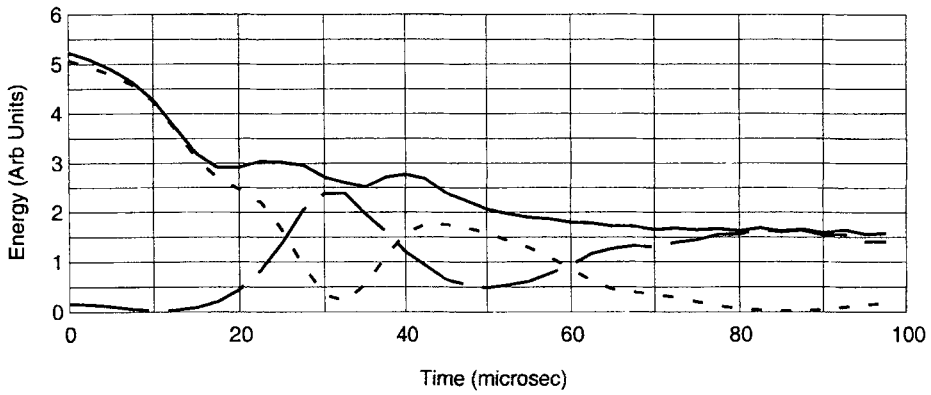

FIGURE 4. Energy in the two modes. The dotted curve is the energy in the $n_z = 1$ mode, the dashed curve is the energy in the $n_z = 2$ mode and the solid curve is the total energy in both modes.

This simple model does not predict that the modes should end up in the final state that we see, with the phase near $\pm\frac{\pi}{2}$ and the $n_z = 1$ mode large and the $n_z = 2$ mode small. To predict how the phase should behave, we need more information.

A more complete model

We need to include the momentum equation to find how the phase should evolve (equivalent to finding the nonlinear frequency shifts). We convert the set of equations (one continuity and one momentum equation for each mode) to second order equations. From this we find a growth rate of

$$\gamma = \left(\frac{3}{4}\right)\frac{n_{20}}{2n_0}\omega_1 \cos\phi \tag{8}$$

for the $n_z = 1$ mode, which is 3/4 of the rate given by Eq. 5 in the earlier model.

When we numerically integrate these coupled equations, we find that phase locking does not occur unless there is damping of the n_z=2 mode. Without damping the modes just convert back and forth indefinitely. With damping, the phase locks near that given by

$$\tan\phi = \frac{2\delta\omega}{\gamma_2} \tag{9}$$

where γ_2 is the damping rate of the n_z=2 mode. Note that for a small γ_2 this will be near $\pm\frac{\pi}{2}$, depending on the sign of $\delta\omega$.

The amplitudes obey the relationship that

$$\frac{n_{20}}{n_{10}^2} = \text{constant} \tag{10}$$

where the constant depends on $\frac{\delta\omega}{\omega_1}$ and $\frac{\gamma_2}{\omega_1}$.

This final state represents a slow decay as energy is slowly fed into the n_z=2 mode from the n_z=1 mode. Since the amplitude of the n_z=2 mode is small, the rate of energy loss is small and this state persists for a long time. Of course this model is also incomplete, as it is an infinite space model and ignores finite-length, image charge, and radial profile effects. It also ignores the damping of the n_z=1 mode. It does, however, seem to capture the essential physics of what is going on in the experiment.

GROWTH OF SOLITONS FROM NORMAL MODES

A soliton is a wave in a dispersive medium that is large enough that nonlinear steepening effects just balance the dispersive spreading, causing it to propagate unchanged. Solitons occur in many physical situations [5].

The cold fluid equations for a plasma in a cylinder can be manipulated, making some assumptions, into the form of the first integral of the Korteweg-deVries equation [6]. This means that these solitons should have the properties of the well known solutions of that equation.

The relevant properties of Korteweg-deVries (KdV) solitons are

1. They travel faster than the linear wave speed in the medium.

2. Two solitons pass through each other basically unaffected, except that their exit times are delayed relative to what you would expect from their initial speeds and entry times. If we just observe their entry time and exit time we would say that their average velocity is less while interacting.

3. The amplitude is linked to a specific speed and width. As the amplitude increases the speed also increases. As the amplitude increases the width decreases.

4. The soliton has the characteristic shape of $\mathrm{sech}^2(z/\Delta)$ where Δ is the width of the soliton.

Solitons can be created in two ways. One is to put a large potential step on a confining ring [7,8]. This requires a relatively large voltage (tens to hundreds of volts.) Another way is to create them from normal modes [6]. Essentially you are repeatedly hitting the pulses at the right time with a small voltage. This second method is the one used to make the solitons in this paper.

The number of solitons created from a given normal mode is equal to n_z and in numerical simulations they have the characteristic sech^2 shape of KdV solitons [6]. Solitons can only be created in a small amplitude range with this method. For the soliton to to remain in phase with the drive, the average speed of the soliton must be equal to the linear wave speed. This requires a balance between the amplitude of the soliton (which affects its speed) and the nonlinear slowing during interactions.

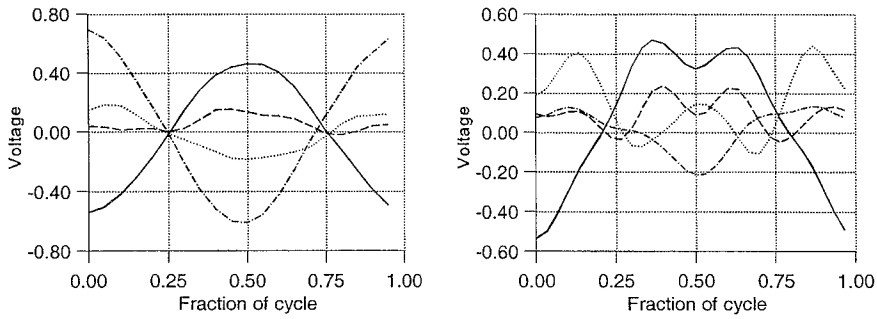

FIGURE 5. Normal Modes and Solitons. The figure on the left shows waveforms on various wall rings when the $n_z = 2$ mode is in its linear state. The figure on the right shows the waveforms when solitons are present in the system.

When the soliton is not interacting, its speed is greater than the linear wave speed, and so the speed can average to the linear wave speed.

Figure 5 shows the waveforms on different sections of the wall both with and without solitons. Without solitons, shown on the left, all the signals have different amplitudes, but the same time dependence. With solitons, as shown on the right, you can see the negative bump of the soliton moving under each ring in sequence. There are also other oscillations visible in this figure that we think are due to external resonances in our system. Assuming that the peaks in the figure occur when the peak of the soliton passes under the center of each ring and knowing where each ring is located allows us to compute the velocity of the soliton. The position as a function of time is shown in Figure 6. This shows that the speed is higher during the short time when the solitons are not interacting either with the ends or with each other.

If we observe these solitons 20 microseconds later, as shown in Figure 7, we see that one of the solitons has disappeared. This disappearance of the soliton is somewhat reminiscent of the mode coupling – the equivalent of the n_z=2 mode has disappeared and been replaced by the equivalent of the n_z=1 mode. When we observe during the time of disappearance, as shown in figure 8, we find that one of the solitons decreases in amplitude and slows down until it is overtaken and appears to be absorbed by the other. The details of how this happens are still unclear. It is possible that a small amount of the linear type $n_z = 2$ normal mode oscillation occurs underneath the solitons. If this mode converts to the $n_z = 1$ mode, one side will be enhanced and the other decreased by that mode. This would cause one side to be smaller and move more slowly. This hypothesis has not yet been investigated in detail, however.

The non-interacting velocity of the single soliton is too high for a cold fluid model of the soliton to explain, but is about what you would expect from a kinetic model [9]. The non-interacting velocity of the two solitons is somewhat higher than that

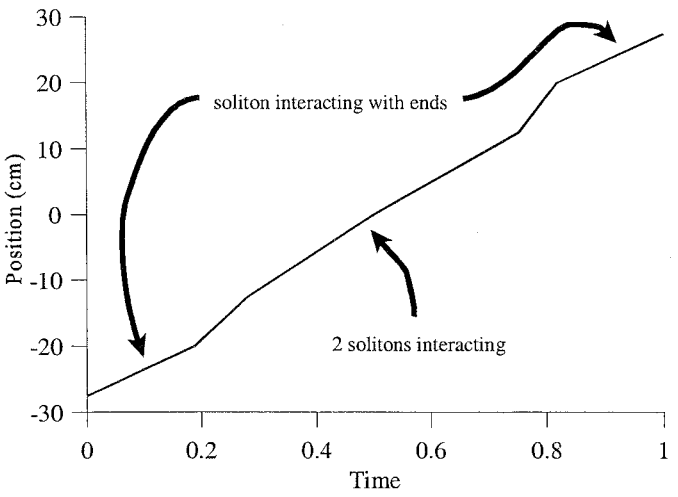

FIGURE 6. Position vs. Time for a soliton when two solitons are in the system.

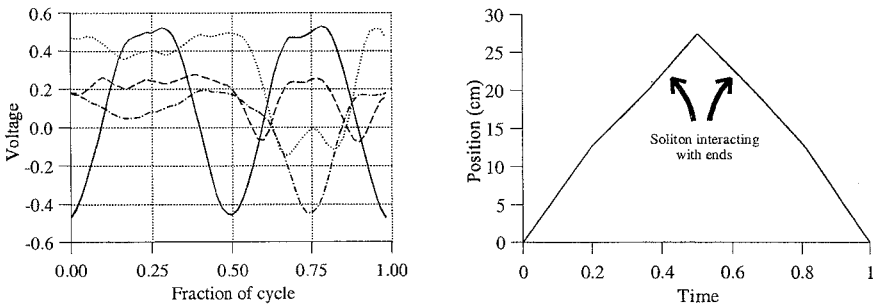

FIGURE 7. One Soliton Signals. The figure on the left shows the waveforms on various wall rings after one of the solitons has disappeared. The cycle referred to on the x-axis label is now twice as long as it is in Figure 5. The figure on the right shows the position vs. time of the one soliton.

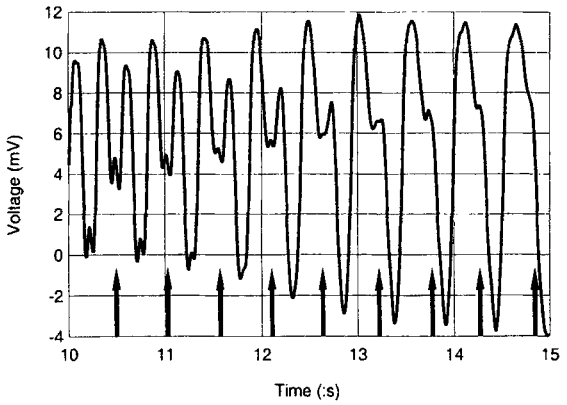

FIGURE 8. Disappearance of One Soliton. One soliton becomes smaller and slower than the other. The arrows indicate the position of the soliton that will disappear.

of the one soliton and cannot yet be fully explained.

CONCLUSIONS

The nonlinear effects of mode coupling, phase locking and soliton formation have all been experimentally observed and most of their properties are as predicted. Some points have not yet been reconciled, including the amplitude dependence of mode coupling, the fact that the free soliton velocity is too high when two solitons exist in the system and the details of how one of the solitons disappears.

REFERENCES

1. deGrassie, J. S. and Malmberg, J. H., *Phys. Rev. Lett.* **39**, 1077 (1972).
2. Hart, G. W. *Phys. Fluids B*, **3**, 2987 (1991).
3. Prasad, S. A. and O'Neil, T. M., *Phys. Fluids* **26**, 665 (1983).
4. Jennings, J. K., Spencer, R. L., and Hansen, K. C., *Phys. Plasmas* **2**, 2630 (1995).
5. Ikezi, H., Barrett, P. J., White, R. B., and Wong, A. Y., *Phys. Fluids* **14**, 1997 (1971) and references contained therein.
6. Hansen, K. C., "The Linear and Nonlinear Stages of the Electrostatic Modes of a Warm, Nonneutral Plasma", Master's Thesis, Brigham Young University (1995).
7. Moody, J. D., and Driscoll, C. F., *Phys. Plasmas*, **2** 4482 (1995).
8. Neu, S. C. and Morales, G. J., *Phys. Plasmas*, **2** 3033 (1995).
9. Rasband, S. N., "Numerical Investigations of Solitons and Holes in a Long Nonneutral Plasma", These proceedings.